scientific reports

Check for updates

OPEN

Kinetics study of sonotransesterification of low grade crude palm oil (CPO) using heterogeneous Na_2O/activated natural mordenite catalyst

Maria Ulfa Nurcahyani, Sumari Sumari✉, Aman Santoso, Galih Satrio Putra, Evilia Wahyuning Nur A'issyah & Ahmat Fanani Hidayatulloh

The kinetics of transesterification have been extensively studied, primarily focusing on conventional heating methods and various catalytic systems. This study addresses a critical gap by investigating reaction kinetic on the sonotransesterification of low grade crude palm oil (CPO) using an activated natural mordenite (ANM) zeolite impregnated with Na_2O catalyst, with the influence of temperature at 45 °C, 55 °C, 65 °C, and 75 °C as well as reaction time of 15 min, 30 min, 45 min, and 60 min. The results demonstrate a maximum biodiesel yield of 80.08% at 65 °C after 60 min of reaction, under conditions of 4% catalyst loading and an alcohol to oil molar ratio of 12:1. However, at higher temperatures, the decline in biodiesel yield was observed, likely due to excessive cavitation effects. Kinetic analysis indicated that the reaction followed a pseudo-first-order kinetic model, with a low activation energy (Ea) of 23.229 kJ/mol, a frequency factor (A) of 7×10^{-3}, and a rate constant (k) of $7 \times 10^{-3}.e^{-23229/RT}$. The notably reduced activation energy demonstrates the catalyst's efficiency in facilitating the reaction under ultrasonic conditions. The decrease in activation energy in biodiesel synthesis using the Na_2O/ANM catalyst provides a good prospect for increasing the productivity and efficiency of the biodiesel industry.

Keywords Biodiesel, Kinetics, Low grade CPO, Zeolite, Sonotransesterification

The increasing global demand for fossil fuels over recent decades has led to the depletion of petroleum reserves and contributed significantly to environmental degradation[1]. This situation has driven researchers to find alternative and renewable energy sources[2]. Among them, biodiesel has emerged as a promising substitute for conventional diesel due to its biodegradability, renewability, and cleaner combustion characteristics[3,4]. Notably, biodiesel contains approximately 11% more oxygen by weight than petrodiesel, which enhances combustion efficiency and reduces particulate emissions[5].

Biodiesel is typically produced via a transesterification reaction between triglycerides and alcohol in the presence of a catalyst. This process generates a long-chain fatty acid methyl ester (FAME) and glycerol as a by-product[6]. However, the economic viability of biodiesel remains a significant challenge, particularly due to the high cost of feedstocks[78]. In this content, the use of Low cost, non-edible, or waste-derived oils with high free fatty acid (FFA) content was being explored[4]. One such source is Low grade Crude Palm Oil (CPO), a by-product of palm oil milling, which contains high levels of FFA, moisture, and other impurities[9]. However, these components interfere with base-catalysed transesterification, making a pretreatment step essential to reduce the FFA content and improve conversion efficiency[10].

Catalyst selection plays a crucial role in biodiesel production[11]. Homogeneous base catalysts such as NaOH[12] and KOH[13] are widely used due to their superior catalytic activity[14]. However, these catalysts are completely soluble in the reaction mixture, making a difficult product separation and generating significant wastewater during the purification process[815],. As an alternative, heterogeneous base catalysts have attracted attention for their environmental friendliness, reusability, and ease of separation[16]. Among these, base metal oxide

Department of Chemistry, Faculty of Mathematics and Natural Sciences, Universitas Negeri Malang, Jl. Semarang 5, Malang, Indonesia. ✉email: sumari.fmipa@um.ac.id

impregnated into zeolite is a promising candidate catalyst, combining zeolites' high thermal stability and surface area with the strong basicity of metal oxides such as Na_2O or K_2O[17].

Natural zeolites stand out due to their abundant availability, thermal resistance, well-defined porous structure and a large surface area[18]. Natural zeolites are classified into several types based on their crystal structure, pore size, and Si/Al ratio. Examples include analcime (ANA), chabazite (CHA), clinoptilolite (HEU), and mordenite (MOR). Among these, mordenite-type natural zeolite is considered one of the most promising due to its relatively large pore size of approximately 0.7×0.65 nm, which makes it suitable for catalytic applications involving large organic molecules[19]. The catalytic activity of zeolites can be further enhanced by acid activation and impregnation with base metal oxides. Acid activation removes structural impurities, increases the Si/Al ratio, and improves textural properties, while metal oxide loading (e.g., Na_2O, K_2O, CaO) introduces basic active sites that facilitate transesterification[20,21].

Several studies have reported high biodiesel yields using such modified zeolite. For instance, Na_2O/K_2O impregnated on activated natural zeolite catalyst proved to be an effective catalyst in the transesterification reaction of kapok seed oil with the highest yield of 85.45%[2]. Other impregnated zeolite catalysts in biodiesel synthesis, such as Na_2O/NaX, also result in a high yield (more than 90%) and a methyl ester conversion of 99.3%[22]. The Li/NaY also catalyst gave a high yield of 98.6%[23]. CaO/Zeolite catalyst also provides a high yield of 90.89%[24]. However, these systems often require long reaction times or high temperatures under conventional conditions.

Ultrasonic irradiation, known as sonotransesterification, has been proposed as a process intensification method due to cavitation effects. Ultrasonic waves generate cavitation effects that significantly enhance mass transfer between immiscible reactants (oil and alcohol), reduce reaction times, and improve yields[25,26]. Wo et al. have reported that reaction time for biodiesel synthesis could be reduced from 360 min (conventional mixing) to just 30 min using ultrasonics[27]. Santoso et al. also demonstrated that ultrasonic cavitation could reduce the reaction time from 120 to 35 min, with a yield of 88.06%[28]. However, excessive cavitation intensity may lead to localised high temperatures and pressures, which could degrade reactants or products through pyrolysis[27].

Evaluating the reaction kinetics of biodiesel synthesis is crucial to support the rational design and optimization of process parameters[29,30]. Furthermore, ultrasonic-assisted transesterification under moderate conditions was used in this study, combined with kinetic modelling and activation energy determination. Kinetic modelling allows researchers to evaluate the efficiency of catalysts, predict reaction behaviour under various conditions, and estimate key parameters such as reaction rate constants and activation energy[7,31]. These insights are crucial when using heterogeneous catalysts and low grade feedstocks, where mass transfer limitations and catalyst reactivity may significantly influence reaction performance.

Despite extensive studies on transesterification kinetics under conventional thermal conditions, limited research has explored kinetic behaviour under ultrasound-assisted systems using natural zeolite-based catalysts. In contrast, this study utilizes natural mordenite that has undergone stepwise acid activation and Na_2O impregnation, resulting in a cost-effective and efficient heterogeneous catalyst. The application of ultrasonic irradiation offers intensified mixing and cavitation effects, which may alter the kinetic pathway compared to conventional approaches.

This study investigated the effect of temperature and reaction time on ultrasonically assisted transesterification of Low Grade Crude Palm Oil (CPO) (Sonotransesterification) using a waterbath sonicator. The Na_2O supported on activated natural mordenite zeolite (ANM) catalyst was used for the transesterification. The catalyst was characterised using XRD, SEM–EDX Mapping, BET, and acidity analysis. Biodiesel yields were compared with SNI 7185:2015 and ASTM D6751 standards to asses quality. The experimental data were then used to determine the most suitable kinetic model. The modelling assumed that methanol was in excess (allowing pseudo-first-order treatment), the reaction system was isothermal, and ultrasound eliminated mass transfer limitations. Based on these assumptions, rate constants and activation energy were calculated using the Arrhenius equation to evaluate the catalytic efficiency and develop a foundation for future process scale-up.

Materials and methods

Materials

Low grade Crude Palm Oil (CPO) was obtained from PT. Sawit Arum Madani, Blitar, East Java, Indonesia. Natural Mordenite zeolite was obtained from South Malang, East Java, Indonesia. All solvents and chemicals, such as HF 48%, HCl 37%, NH_4Cl, H_3PO_4 85%, H_2SO_4 95%, methanol (p.a ≥ 99.9%), and aqua demineralization, are analytical grade and can be used without purification. All chemicals were purchased from Sigma Aldrich (commercial sources).

Natural zeolite activation

Natural zeolite was first ground and sieved to a particle size of 100 mesh. The sieved zeolite was washed thoroughly with distilled water to remove surface impurities and dried in an oven at 120 °C for 2.5 h. The dried zeolite was calcinated at 500 °C for 4 h in a muffle furnace to eliminate volatile matter and improve thermal stability. The calcined zeolite was treated with a 1% hydrofluoric acid (HF) solution at 1:2 (w/v). The mixture was stirred for 30 min at room temperature to partially dissolve amorphous silica and open up the pore structure. After treatment, the zeolite was filtered and washed with distilled water until reaching neutral pH, and then dried again at 120 °C for 2.5 h. Next, the HF-treated zeolite was refluxed with a 6 M hydrochloric acid (HCl) solution at a 1:2 (w/v) ratio for 5 h at 60 °C to further remove extraneous cations (e.g., Ca^{2+}, Mg^{2+}, Fe^{3+}) and enhance the Si/Al ratio. After refluxing, the sample was filtered and washed with distilled water until reaching neutral pH, and then dried at 120 °C for 2.5 h.

The acid-treated zeolite was then subjected to ion exchange using a 1 M ammonium chloride (NH_4Cl) solution at a 1:2 (w/v) ratio. The mixture was stirred on a shaker at 150 rpm for 2 h at room temperature. The

exchanged zeolite was filtered and washed repeatedly with distilled water to remove excess ions, and dried at 120 °C for 2.5 h. Finally, the fully treated zeolite was calcined at 500 °C for 4 h to convert the ammonium form (NH_4^+-Zeolite) into the protonic form (H^+-Zeolite) and stabilise the structure. The resulting material is called activated natural mordenite (ANM) and was further characterised using XRF, XRD, SEM, BET, and acidity analysis.

Catalyst preparation and characterisation

The Na_2O/ANM catalyst was synthesised through the impregnation method, based on Naik et al. and Arni et al.'s research[17,32]. Activated natural zeolite is mixed into 30% NaOH with a ratio of 1:4 (w/v). The mixture is then stirred using a waterbath shaker for 12 h at 130 rpm. After 23 h, the mixture is transferred to a petri dish and gently dried in the oven at 110 °C for 4 h. The catalyst is then calcined at 450 °C for 4 h. Prepared catalysts were analysed using XRD, SEM–EDX Mapping, BET, and acidity analysis. Figure 1 shows the preparation process of Na_2O/ANM catalysts.

Catalyst acidity characterisation

The method used to characterise the acidity of the catalyst refers to and Sumari et al.[37] with a modification. Each of the activated natural mordenite (ANM) and Na_2O/ANM catalyst samples was weighed to approximately 0.300 g and placed on a pre-weighed watch glass. The samples were then introduced into a vacuum desiccator, which had been pre-saturated with concentrated ammonia solution for 24 h. The amount of adsorbed ammonia was calculated based on the difference in sample mass before and after ammonia adsorption, using the following equations:.

$$\text{Adsorbed ammonia (mol)} = \frac{(b - a)}{\text{molecular weight of } NH_3}$$

$$\text{Total acidity } \left(\frac{\text{mol}}{\text{g}}\right) = \frac{\text{mole of absorbed ammonia}}{a}$$

where a is the mass of the sample before ammonia adsorption (g) and *b* is the mass of the sample after ammonia adsorption (g).

Low grade CPO preparation and characterisation

Low grade CPO preparation consists of three main stages: refining using bleaching earth, degumming, and esterification, adapted from Gharby et al. with slight modifications[33]. In the refining stage, the crude CPO was heated to 100 °C and mixed with 20% (w/b) bleaching earth. The mixture was stirred using a mechanical stirrer at 400 rpm for 1 h at 170 °C. After refining, the oil was filtered and collected for further treatment. In the degumming stage, the refined oil was heated to 70 °C and treated with 0.3% (v/v) phosphoric acid (H_3PO_4), followed by magnetic stirring at 70 °C for 30 min. The mixture was then cooled and centrifuged at 3000 rpm for 15 min to remove gums. The oil was washed with warm distilled water and reheated to 90–100 °C.

The esterification stage was conducted to reduce the free fatty acid (FFA) content. The degummed oil was refluxed for 4 h at 60–65 °C under constant stirring, with an oil: alcohol ratio of 1:12 and 1% (w/b) sulfuric acid (H_2SO_4) catalyst. Afterwards, the mixture was transferred to a separatory funnel and allowed to stand for 24 h to separate into two layers. The bottom layer was removed, and the upper layer (esterified oil) was washed with warm water, dried at 90–100 °C, and treated with anhydrous $MgSO_4$ to remove residual moisture. To ensure the

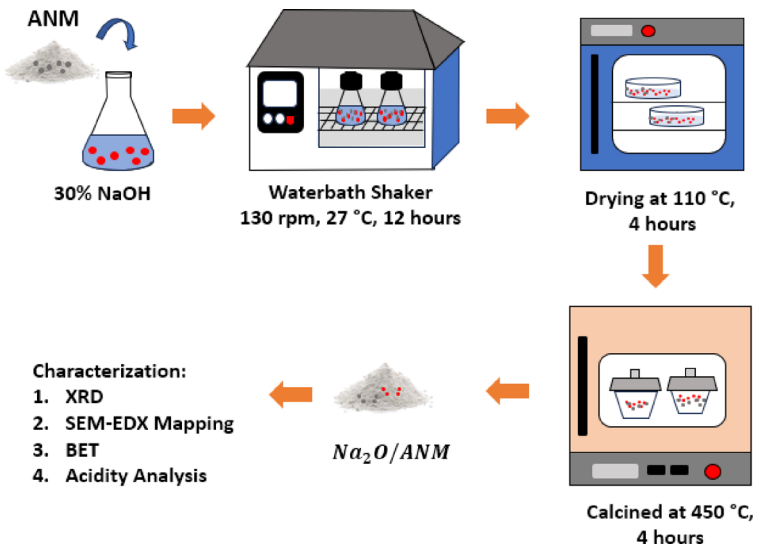

Fig. 1. Na_2O/ANM catalyst preparation procedure.

efficiency of each pretreatment step, density, viscosity, refractive index, and free fatty acid (FFA) content were measured after each stage (refining, degumming, and esterification).

The determination of FFA was performed using a standard acid–base titration method. A total of 1.00 g of the oil sample was weighed into a conical flask, followed by adding 5 ml of 95% ethanol and three drops of phenolphthalein indicator. The mixture was titrated with standardised 1 N potassium hydroxide (KOH) solution until a stable pale pink colour appeared. The FFA content was calculated using the following equation:

$$\mathrm{FFA}(\%) = \frac{\mathrm{v\ KOH\ x\ N\ KOH\ x\ MW}}{\mathrm{w\ x\ 1000}}\ \mathrm{x\ 100\ \%}$$

where,

- V_{KOH} = volume of KOH used (mL)
- N_{KOH} = normality of KOH (N)
- MW = average molar mass of free fatty acids
- W = mass of oil sample (g)

Unless otherwise specified, the average molar mass (Mr) used corresponds to oleic acid. The resulting FFA percentage indicated oil quality for each processing stage.

Ultrasonic-assisted transesterification of low grade CPO using waterbath sonicator

25 g of Low Grade Esterified CPO was put into the Erlenmeyer and heated to a temperature of 40 °C. Low grade CPO is then poured into a mixture of alcohol and 4% Na_2O/ANM catalyst that has been heated at 65 °C by waterbath sonication at 37 kHz for 2 min, with the molar ratio of oil and alcohol of 1:12. The mixture of oil, alcohol, and catalyst are shaken and then heated in an Waterbath sonicator with a temperature and time variation as can be seen in Fig. 2. After that, the mixture was centrifuged (3000 rpm) for 15 min to separate the catalysts.

The liquid product mixture is put into a separate funnel until it forms two layers. The top layer is washed using warm water and then heated (90–100 °C. The heated biodiesel is added with anhydrous $MgSO_4$ to bind the water residues. The resulting biodiesel was analysed for density, viscosity, refractive index, free fatty acid content, saponification value, and calorific value.

Kinetic study in sonotransesterification of low grade CPO

Reaction kinetics studies determine the rate constants and activation energy in the sonotransesterification of low grade CPO. The transesterification reaction was carried out at 45 °C, 55 °C, 65 °C, and 75 °C with 15, 30, 45, and 60 min. Other parameters that are considered constant include ultrasonic frequency (37 kHz), number of catalysts (4% b/b), and oil: alcohol molar ratio of 1:12. Determination of the kinetic model of the sonotransesterification reaction low grade CPO is carried out by looking for the highest correlation coefficient (R^2) of the graph of zero, first, and second order reactions. The reaction equation used in the kinetics study of transesterification reactions is simplified to one direction, as in previous studies[23,34,35].

Triglyceride [A] + 3 Methanol [B] → 3 Fatty Acid Methyl Ester [C] + Glycerol [D].

The rate equation for zero-order reactions is written in Eq. (1).

$$r_A = -\frac{d[A]}{dt} = k \tag{1}$$

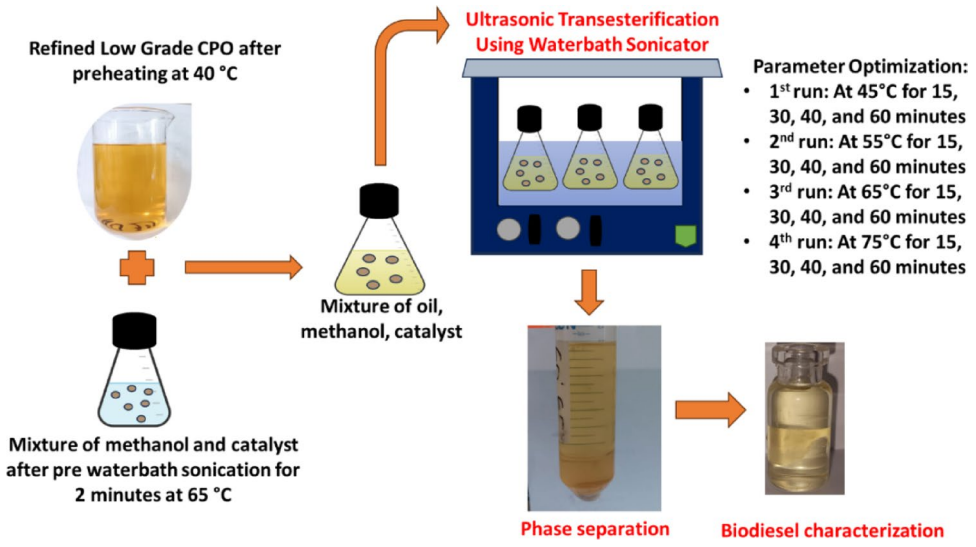

Fig. 2. Sonotransesterification procedure of low grade CPO Na_2O/ANM Catalyst.

Equation (1) can be transformed into its integral form, resulting in Eq. (2). Equation (2) is a straight-line y = a + bx equation. y is [A], a is $[A_0]$, b is k, and x is t. The values y, a, and b in the equation can be obtained by making a graph [A] against time with a slope value of -*k*.

$$\int_{A0}^{A} d[A] = -\int_{0}^{t} kdt$$
$$[A] - [A_0] = -kt$$
$$[A] = -kt + [A_0] \tag{2}$$

The concentration of triglycerides formed per unit of time [A] can be calculated based on the biodiesel yield at each temperature and time variation using Eq. (3).

$$[A] = [A_0] - \frac{1}{3}[C] \tag{3}$$

The rate equation for the first-order reaction is written in Eq. (4).

$$r_A = -\frac{d[A]}{dt} = k[A] \tag{4}$$

Equation (4) can be transformed into its integral form with the result as in Eq. (5).

$$\int_{A_0}^{A} \frac{1}{[A]} d[A] = -\int_{0}^{t} kt$$
$$\ln\frac{[A]}{[A_0]} = -kt$$
$$\ln[A] - \ln[A_0] = -kt$$
$$\ln[A] = -kt + ln[A_0]$$
$$\ln k = \ln A - \frac{Ea}{R}\frac{1}{T} \tag{5}$$

Equation (5) is a straight-line y = a + bx equation. Variable y is the coordinate ln [A], variable a is intercept ln $[A_0]$, variable b is slope -k, and variable x is abscess t. The values y, a, and b in the equation can be obtained by making a graph between ln [A] vs time (minutes), with a slope of -k.

Furthermore, the reaction rate equation for second-order reactions is shown in Eq. (6), with [A] ≠ [B].

$$r_A = -\frac{d[A]}{dt} = k[A][B] \tag{6}$$

If it is known, then Eq. (7) will be obtained

$$[A] = [A_0] - x[B] = [B_0] - x$$
$$-\frac{dx}{dt} = -k([A_0] - x)([B_0] - x)$$
$$\frac{dx}{([A_0] - x)([B_0] - x)} = kdt \tag{7}$$

Equation (7) can be transformed into its integral form, resulting in Eq. (8).

$$\int_{0}^{x} \frac{dx}{([A_0] - x)([B_0] - x)} = k\int_{0}^{t} dt$$
$$\frac{1}{[B_0] - [A_0]}\left[\int \frac{dx}{([A_0] - x)} - \frac{dx}{([B_0] - x)}\right] = k\int_{0}^{t} dt$$
$$\frac{1}{[B_0] - [A_0]}\left(\ln\frac{[A_0]([B_0] - x)}{[B_0]([A_0] - x)}\right) = kt$$
$$ln\frac{[A_0]([B_0] - x)}{[B_0]([A_0] - x)} = ([B_0] - [A_0])kt$$
$$ln\frac{[A_0]}{[B_0]} + ln\frac{[B_0] - [A_0]x}{[A_0] - [B_0]x} = ([B_0] - [A_0])kt$$

$$ln\frac{[B_0]-[A_0]x}{[A_0]-[B_0]x} = ln\frac{[B_0]}{[A_0]} + ([B_0]-[A_0])kt \tag{8}$$

Equation (8) is a straight-line y = a + bx equation. Variable y is the coordinate $ln\frac{[B_0]-[A_0]x}{[A_0]-[B_0]x}$ variable a is the intercept $ln\frac{[B_0]}{[A_0]}$. Variable b is the slope $([B_0]-[A_0])k$, and variable x is abscess t. The regression curve analysis on the three reaction models produced the largest regression value of R^2, which was used to determine the activation energy value (E_a) according to the Arrhenius equation in Eq. (9).

$$k = Ae^{\frac{-Ea}{RT}} \tag{9}$$

Arrhenius' equation can be written as a logarithmic Eq. (10).

$$\ln k = \ln A - \frac{Ea}{R}\frac{1}{T} \tag{10}$$

Equation (10) is a straight-line y = a + bx equation. The values y, a, and b in the equation can be obtained by making a graph between ln k vs 1/T, where y is ln k, a is ln A, b is $-\frac{Ea}{R}$, and x is $\frac{1}{T}$.

Results and discussion

Characterization of activated natural mordenite zeolite (ANM)

The natural zeolite used in this study was obtained from South Malang, Indonesia. Natural zeolites have different compositions and crystallinity, depending on their geological source. A pre-treatment process involving washing, acid activation, and ion exchange was performed to enhance consistency and remove impurities[2,36]. The activation of natural zeolite in this study was carried out physically and chemically. Physically, zeolite activation is carried out by grinding, sifting, and heating zeolite at high temperatures. Physical activation aims to separate impurities, obtain uniform size, and increase the surface area of zeolite[37]. The zeolite that has been physically activated changes colour from green to brown as shown in Fig. 3a, b, due to the oxidation of Fe^{2+} ions to Fe^{3+} after calcination. In addition, the activation process can lead to zeolite dehydration, followed by increased Fe oxide levels, which causes the zeolite to darken in colour[37].

Chemical activation was performed by dispersing zeolite into HF and HCl solutions to reduce zeolite's free silica, alumina, and metal contaminants and increase the pore size of zeolite[2]. The reduction of metal contaminants is characterised by a change in zeolite colour from brown to pale yellow, as shown in Fig. 3c. These results are consistent with those reported in previous studies[2,38]. Meanwhile, the activation with NH_4Cl aims to exchange the charge-balancing metal of the zeolite framework with ammonium ions (NH_4^+) from NH_4Cl. The ammonium ions will be released as NH_3 gas through heating at high temperatures (500 °C) so that H-Zeolite is obtained[38,39].

Table 1 provides the chemical analysis by using XRF. It is noticed that Natural Zeolites contain impurity atoms such as Fe, Ti, Mn, Cu, Zn, with a total of above 26%. These atoms originated from the impurities in the mineral in natural zeolite. The XRF result indicates that after the chemical activation process with acids, the percentage of impurity metal oxides, such as Fe, is decreased from 25.6% to 4.41%. The decrease of metal impurity was followed by an increase in the Si/Al ratio in zeolite from 6.48 to 8.9[40]. This result is in good agreement with the previous report that the natural mordenite zeolite is silica-rich[2,26]. An increase in the Si/Al ratio can improve the stability of zeolite at high temperatures, and also can increase the acidity of zeolite[41,42].

Natural zeolite commonly consists of multiple zeolitic phases, including Analcime, Clinoptilolite, Faujasite, Mordenite, and others, which are greatly influenced by the zeolite's origin. Therefore, X-ray diffraction (XRD) characterisation is needed to determine the type of zeolite present in the natural zeolite used in this study. Figure 4 depicts the XRD profile of the Activated Natural Zeolite obtained from South Malang, Special Region of Jawa Timur, Indonesia. The XRD profile indicated that mordenite is the primary structure of the Activated Natural Zeolite. The mordenite peaks appeared at 2θ = 13.44°, 22.2°, 25.62°, 26.24°, and 27.66° (COD ID 9005607). This result agrees with the previous report on using zeolite obtained from South Malang, Jawa Timur,

Fig. 3. (**A**) Natural mordenite before activation, (**B**) Natural mordenite after physical activation, (**C**) Natural mordenite after chemical activation (ANM).

Before activation		After activation	
Elements	Percentage (%)	Elements	Percentage
Si	48.6	Si	71.7%
Al	7.5	Al	8.0%
K	3.35	K	3.49%
Ca	11.3	Ca	10.2%
Ti	1.65	V	0.01%
V	0.074	Ti	1.51%
Cr	0.070	Cr	–
Mn	0.37	Mn	0.080%
Fe	25.6	Fe	4.41%
Cu	0.17	Cu	0.088%
Zn	0.06	Zn	–
Sr	0.66	Sr	0.42%
Eu	0.3	Eu	0.1%
Re	0.2	Re	–

Table 1. XRF natural zeolite before activation and after activation.

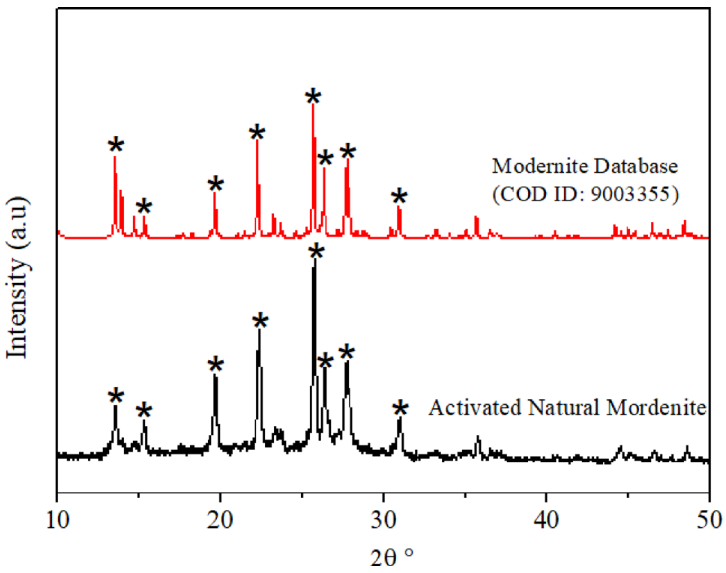

Fig. 4. XRD Activated natural mordenite zeolite and standard mordenite database.

Indonesia[2,38]. The highest typical peak of mordenite is shown at 2θ = 25.62° and 27.66° (JCPDS: 700232). These results suggest that the activation process does not cause crystallinity damage to zeolites, consistent with those reported in previous studies[2].

Characterisation of Na_2O/activated natural mordenite (ANM) catalyst

Na_2O/Activated Natural Mordenite (ANM) catalyst samples were characterised to analyse their physicochemical properties using XRD, SEM–EDX Mapping, BET, and Acidity Analysis.

XRD analysis

The results of XRD analysis of Na_2O/ANM catalyst samples are shown in Fig. 5. The catalyst diffractogram shows that activated natural mordenite zeolite impregnated with metal oxide Na_2O retains the specific peaks typical of activated natural zeolite with high intensity in 2θ = 25.63°. Some of the typical peaks of zeolite appear to have decreased in intensity, as shown at 2θ = 13.45°. It is possible due to the distribution of Na_2O particles and the presence of amorphous Na_2O particles. The impregnated Na_2O particles are also dispersed into the zeolite frameworks so that at the time of XRD testing, the Na_2O peaks become shallow and undetectable on the catalytic diffraction pattern. This result is in line with the findings reported by Sumari et al. and Kusuma et al., who synthesize activated natural zeolite impregnated with K_2O[17,43]. Overall, the catalytic diffraction pattern shows that the activated natural zeolite (ANM) does not undergo significant structural changes after the impregnation process[2,22,44].

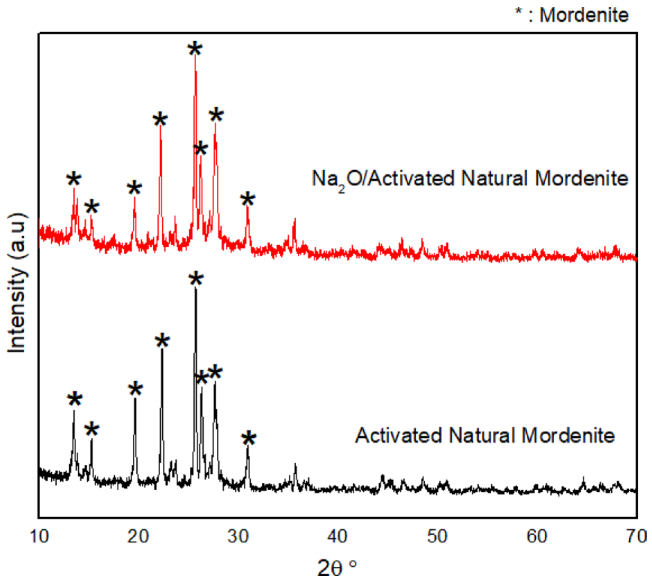

Fig. 5. XRD results of activated natural mordenite before and after impregnation with Na_2O.

Sample	Surface area (m^2/g)	Pore volume (cm^3/g)	Pore diameter (nm)
ANM	240.7	0.14	2.46
Na_2O/ANM	55.78	0.05	3.66

Table 2. Results of BET full-isotherm activated natural mordenite before and after impregnation with Na_2O.

BET analysis

The Brunauer–Emmett–Teller (BET) method, based on N_2 gas adsorption–desorption, was used to measure specific surface area and zeolite pore size before and after Na_2O impregnation. Results of BET's analysis in Table 2 showed that after the impregnation, the activated natural decreased its specific surface area from 240.7 m^2/g to 55.78 m^2/g and its total pore volume from 0.19 cm^3/g to 0.05 cm^3/g. Wu et al. have reported a similar result that Y zeolite experienced a decrease in surface area and total pore volume after impregnation with CaO metal oxide[45].

A decrease in the specific surface area and pore volume of zeolite can occur due to the filling of zeolite pores by metal oxide Na_2O[46]. The results of BET measurements also showed that the pore diameter of zeolite increased along with Na_2O impregnation from 2.46 to 3.66 nm. An increase in pore size can occur due to the reduction of amorphous aluminosilicate and the partial destruction of small zeolite cages due to alkaline treatment[47]. These results show that the metal oxide Na_2O has been successfully impregnated into the pores and surface of the zeolite.

SEM–EDX mapping analysis

The analysis using SEM–EDX Mapping (*Scanning Electron Microscopy with Energy Dispersive X-ray)* was used to observe the morphological changes and distribution of Na_2O particles in activated natural mordenite zeolite. The SEM image of natural mordenite zeolite (Fig. 6a) at 10,000 × magnification shows irregular morphology. This phenomenon occurs due to metal oxides of impurities left over during activation, as reported in previous studies[2]. However, after impregnation with Na_2O, SEM images of the catalyst at 50,000 × magnification (Fig. 6b) show that the zeolite appears agglomerated and exhibits a different morphology from the activated natural zeolites. However, similar results have been reported that the morphology of zeolite impregnated with KOH can turn amorphous due to the partial collapse of the structure of mordenite zeolite[48].

The presence of impregnated Na_2O in activated natural mordenite zeolite is confirmed by SEM–EDX Mapping of the catalysts as shown in Fig. 7. The results show that the Na_2O particles are fairly evenly distributed on the surface of the zeolite, indicated by the green colour area with a percentage of Na element of 15.6% of the total weight. It indicates that the process of Na_2O impregnation has been successfully carried out, as has been reported in previous studies[2,32].

Acidity analysis of the Na_2O/ANM catalyst

The acidity analysis aims to quantify the number of acidic sites using a gravimetric method through ammonia adsorption under vacuum conditions in a desiccator pre-saturated with ammonia vapor. The acidity result of the Na_2O/ANM catalyst and Activated Natural Mordenite (ANM) was presented in Table 3**.**

As shown in Table 3, the amount of adsorbed basic ammonia adsorbed by Activated Natural Mordenite (ANM) after impregnation with Na_2O is significantly lower than before. This indicates that the acidic sites on

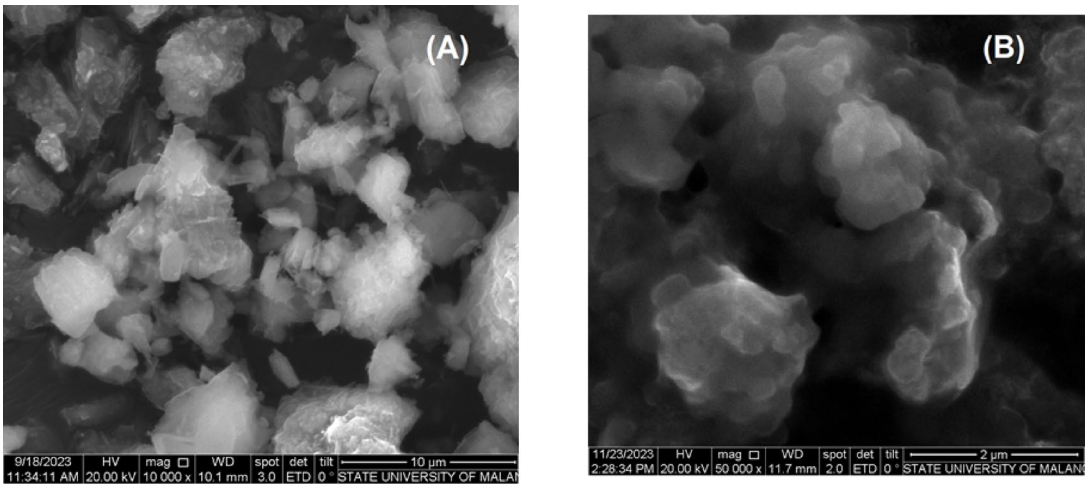

Fig. 6. SEM results (**a**) Activated natural mordenite zeolite (ANM), (**b**) Na_2O/ANM.

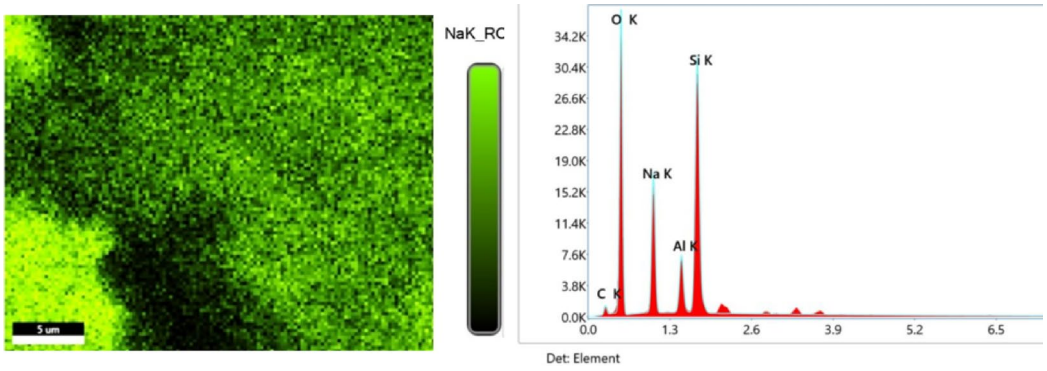

Fig. 7. SEM–EDX mapping results of Na_2O/activated natural mordenite catalyst.

Sample	Mass before ammonia adsorption (g)	Mass after ammonia adsorption (g)	Adsorbed ammonia (mol)	Total acidity (mol/g)
Activated natural mordenite (ANM)	0.5751	0.305	0.813	2.605
Na_2O/ANM	0.3317	0.414	0.082	0.248

Table 3. Results of acidity analysis.

ANM were largely replaced by strong basic sites due to the incorporation of Na_2O. That process reduces the number of acidic sites that are available to interact with basic ammonia, thereby decreasing the catalyst's acidity and increasing its basicity.

CPO pretreatment and characterization

The low grade crude palm oil (CPO) used in this study was obtained from PT. Sawit Arum Madani, located in Blitar, East Java, Indonesia. This oil exhibited typical characteristics of degraded feedstock, including a thick, margarine-like texture, a strong odor, and a yellow orange color, as shown in Fig. 8a. In addition, the low grade CPO contained a high level of free fatty acids (approximately 20%) and exhibited a very high kinematic viscosity of 18.83 cSt, which is unsuitable for direct use in biodiesel production. To enhance its quality and make it more suitable as a biodiesel feedstock, the low grade CPO underwent three sequential pretreatment steps: refining, degumming, and esterification.

The refining process was carried out using bleaching earth to remove impurities, reduce color intensity, and minimize the unpleasant odor. Solid adsorbents such as bleaching earth are often preferred over other materials like activated carbon due to their lower cost and relatively high adsorption capacity[33]. After the refining process, the oil turned cloudy yellow in appearance, as shown in Fig. 8b, and no longer emitted a strong odor. These changes indicate the effective removal of volatile impurities and pigments, consistent with previous findings[49].

Despite the improvement, the refined oil still appeared slightly opaque as shown in Fig. 8b, indicating the possible presence of phospholipids and gum-like impurities. Therefore, a degumming process was carried out

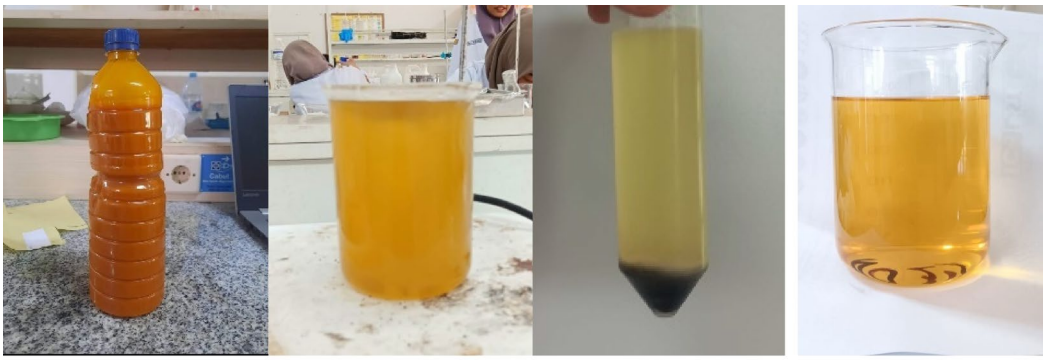

Fig. 8. (**a**) low grade CPO before the pretreatment process, (**b**) The refined low grade CPO, (**c**) The degummed low grade CPO, (**e**) The esterified low grade CPO.

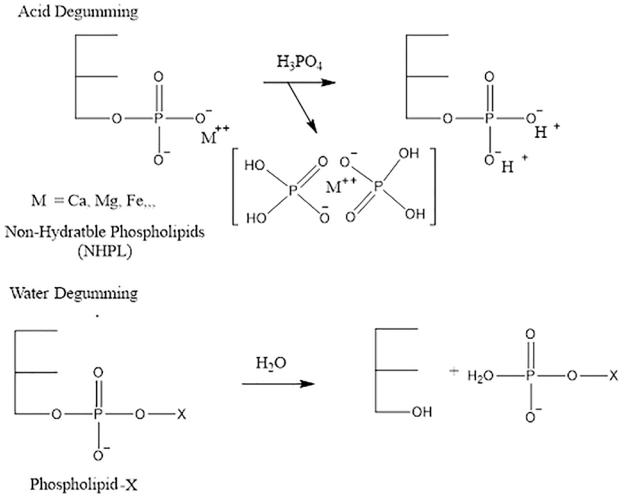

in two steps: acid degumming using a phosphate compound and water degumming. Acid degumming was performed to remove non-hydratable phospholipids by adding phosphoric acid. The acid acts by coagulating non-hydratable phosphatides along with metal ions present in the oil[33]. Acid degumming is typically followed by water degumming to remove hydratable gums (Kulkarni dkk[50].). The reaction mechanism of acid degumming using phosphoric acid is illustrated bellow[51]:.

Following this treatment, the oil exhibited improved clarity, and a dark-colored gum was visibly separated and settled at the bottom of the container as shown in Fig. 8c, confirming the successful removal of polar contaminants. However, the degummed low grade CPO still had a high free fatty acid (FFA) content (approximately 18%) and exhibited a very high kinematic viscosity of 17.02 cSt, considering unsuitable for direct use in biodiesel production. To reduce the FFA for base-catalyzed transesterification, an esterification step was carried out. The esterified low grade CPO exhibited a significant reduction in free fatty acid (FFA) content, from 20 to 2.04%, which meets the acceptable limit for base-catalyzed transesterification. In addition, the oil became noticeably clearer as shown in Fig. 8d and free from strong odors. These results indicate that the pretreatment of low grade CPO was successfully carried out.

Process optimization in sonotransesterification of low grade CPO with Na_2O/ANM catalyst

The process of transesterification is carried out with the help of ultrasonic waves using a 37 kHz waterbath ultrasonic. The transesterification reaction begins with the withdrawal of methanol protons by the metal oxide Na_2O impregnated in zeolite, further producing anions methoxide. The methoxide anion then attacks the C carbonyl atom on the triglyceride, forming a carbonyl alkoxy intermediate. This process continues until 3 mol of methyl ester are obtained[52]. The final product of methyl ester can be seen in Fig. 9.

The highest yield was obtained at a reaction temperature of 65 °C for 60 min, which was 80.08%. At higher temperatures (> 65 °C), the yield of biodiesel appears to decrease because some of the methanol has evaporated at 75 °C, considering that the boiling point of methanol is 64.7 °C[53,54]. Moreover, at higher temperatures, the cavitation effect generated by ultrasonic waves can be weakened, followed by a decrease in biodiesel yield[7]. The biodiesel yields also experienced an increasing trend along with the increase in reaction time, as shown in Fig. 10.

After obtaining the characterization results, the biodiesel obtained is compared with SNI 7185:2015 and ASTM D6751 biodiesel. Table 4 shows that most of the biodiesel obtained from the Sonotransesterification of

Fig. 9. Sonotransesterification results of Na_2O/ANM catalysed low grade CPO.

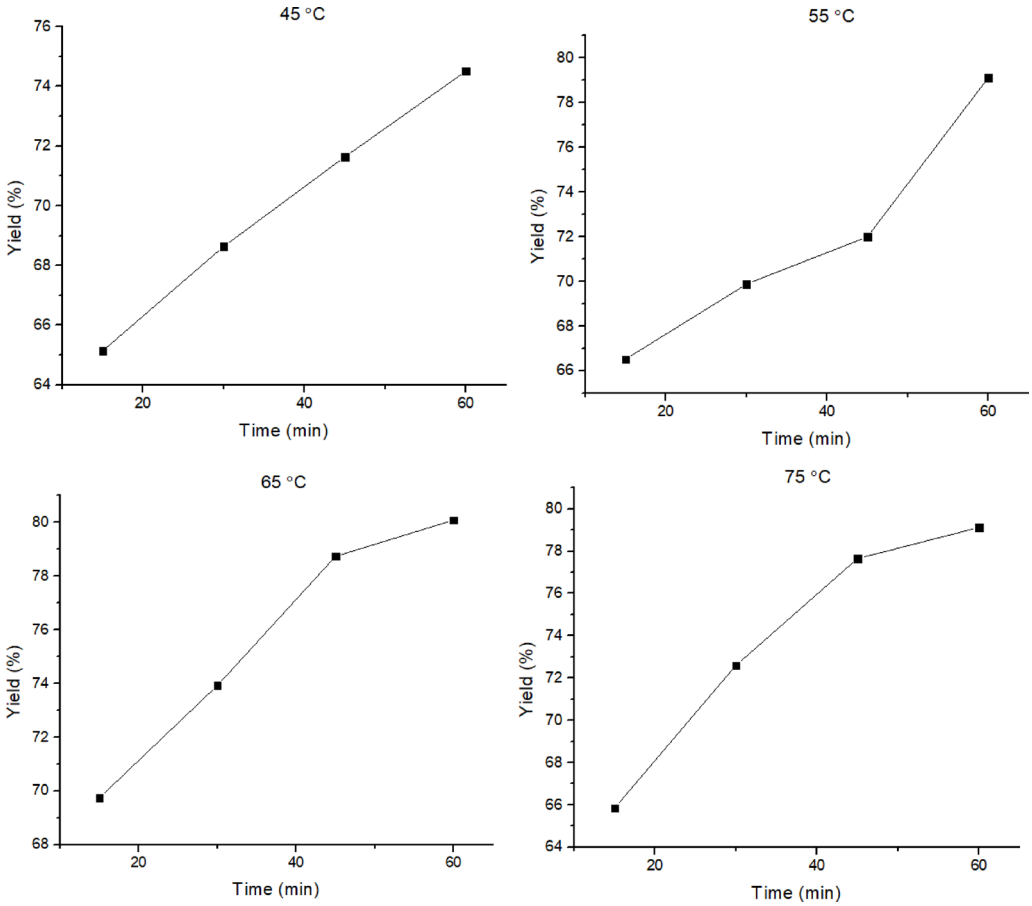

Fig. 10. The effect of time on biodiesel yield at temperature: (**a**) 45 °C, (**b**) 55 °C, (**c**) 65 °C, (**d**) 75 °C.

low grade CPO with Na_2O/ANM catalysts has density, viscosity, refractive index, and free fatty acid content that meet the SNI 7182:2015 and ASTM D6751 biodiesel standards.

The catalytic performance of Na_2O/activated natural mordenite (Na_2O/ANM) in the Sonotransesterification of low grade crude palm oil was evaluated and compared with similar studies in the literature, as shown in Table 5. The highest biodiesel yield obtained in this study was 80.08% at 65 °C for 60 min using a 4 wt% catalyst loading, 1:12 methanol-to-oil molar ratio, and ultrasonic irradiation at 37 kHz. This yield is comparable to

Catalyst	Time (minutes)	Temperature (°C)	Yield (%)	Density(kg/m^3)	Viscosity (Cst)	FFA (%)
SNI 7185:2015				850–890	2.3–6.0	< 0.5
ASTM D6751				820–900	1.6–5.8	< 0.45
Na_2O/ANM	60	75	79.12	879	3.1	0.35
		65	80.08	881	3.5	0.35
		55	79.12	885	3.3	0.59
		45	74.51	807	3.1	0.57
	45	75	77.65	885	3.2	0.35
		65	78.73	882	3.4	0.33
		55	72.00	879	3.5	0.35
		45	71.64	894	3.5	0.32
	30	75	72.60	890	3.2	0.34
		65	73.93	882	3.4	0.34
		55	69.88	887	3.4	0.59
		45	68.64	881	3.5	0.59
	15	75	65.85	885	3.1	0.56
		65	69.74	890	3.4	0.57
		55	66.51	809	3.5	0.24
		45	65.14	896	3.3	0.34

Table 4. Characterization of the results of the sonotransesterification of low grade CPO.

No	Catalyst	Feedstock	Molar ratio (Oil:MeOH)	Catalyst loading (wt%)	Temp (°C)	Time (min)	Yield (%)	Reference
1	**Na_2O/ANM** (This study)	Low grade CPO	1:12	4	65	60	80.08	Present study
2	Na_2O/NaX	Sunflower oil	1:10	5	60	120	76.0	[22]
3	Li/NaY	Soybean oil	1:12	4	65	180	98.6	[23]
4	CaO/Zeolite	Waste lard	1:15	6	70	90	90.89	[24]
5	K_2O/ANM	Kapok seed oil	1:12	4	65	60	85.45	[2]
6	K_2O/Al_2O_3 (Ultrasound)	Off-grade CPO	1:15	3	60	35	88.06	[26]

Table 5. Comparison of biodiesel yield using various zeolite-based catalysts in transesterification.

or even superior to several previous studies utilizing solid base catalysts.For instance, Martínez et al. (2014) reported a biodiesel yield of 76% using a Na_2O/NaX catalyst under conventional heating for 2 hours[23]. Similarly, Li et al. (2019) achieved a higher yield of 98.6% using a Li/NaY zeolite catalyst, but under more severe conditions and longer reaction time[23]. Compared to conventional zeolites, the Na_2O/ANM catalyst demonstrates a good balance between reaction efficiency and mild operating conditions, particularly when combined with ultrasonic irradiation.

The enhanced performance can be attributed to the increased basicity of the catalyst due to Na_2O impregnation and to the structural advantages of activated mordenite, such as improved surface area and pore accessibility. The acid activation process, which included HF and HCl treatment followed by ion exchange with NH_4Cl, significantly improved the physicochemical properties of the zeolite. This is reflected in the increased Si/Al ratio (from 6.48 to 8.9), enhanced crystallinity (as shown by XRD), and reduced metal impurities (confirmed by XRF analysis). These modifications play a critical role in improving the interaction between the Na_2O active phase and the zeolite support, thereby enhancing the basicity and catalytic performance. In comparison, Martínez et al. (2014) reported a lower biodiesel yield of 76% using a Na_2O/NaX catalyst without prior zeolite activation under conventional heating conditions[22], while Li et al. (2019) achieved a higher yield of 98.6% with a Li/NaY catalyst, but under more complex synthesis conditions and longer reaction times[23].

Furthermore, the application of ultrasound significantly improves mass transfer between the immiscible phases, reducing reaction time and enhancing yield, a trend similarly observed by Pukale et al.[7] in ultrasound-assisted transesterification using heterogeneous catalysts[7]. Overall, the combination of low cost catalyst, moderate reaction conditions, and ultrasonic activation positions Na_2O/ANM as a promising candidate for sustainable biodiesel production. This result demonstrates that the Na_2O/ANM catalyst has promising transesterification activity under moderate reaction conditions. Compared to non-activated natural zeolites or unmodified supports used in previous studies, the acid-activated mordenite support in this work contributes to a more favorable catalytic environment.

Analysis using GC–MS showed the presence of several peaks of major components in methyl esters obtained from the sonotransesterification of low grade CPO, as shown in Fig. 11. The chromatogram shows nine peaks, which represent the compounds of methyl ester obtained. Each peak has its retention time and area, as shown

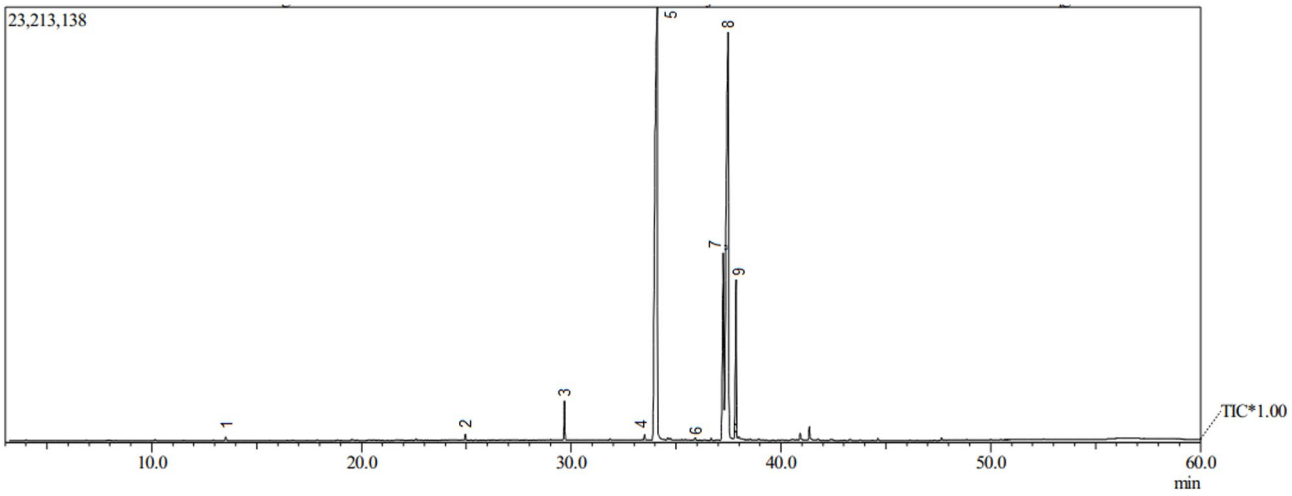

Fig. 11. Chromatogram GC–MS methyl ester.

Peak	tR (min)	Compound name	Formula	%Area	LIB
1	13.251	Methyl octanoate	$C_9H_{18}O_2$	0.14	WILEY229. LIB
2	24.951	Methyl dodecanoate	$C_{13}H_{26}O_2$	0.22	WILEY229. LIB
3	29.679	Methyl tetradecanoate	$C_{15}H_{30}O_2$	1.38	WILEY229. LIB
4	33.500	Methyl-9-hexadecanoate	$C_{17}H_{32}O_2$	0.21	NIST62. LIB
5	34.097	Methyl hexadecanoate	$C_{17}H_{34}O_2$	43.44	NIST12. LIB
6	35.914	Methyl heptadecanoate	$C_{18}H_{36}O_2$	0.11	WILEY229. LIB
7	37.251	Methyl-9.12-octadecadienoate	$C_{19}H_{34}O_2$	10.86	NIST62. LIB
8	37.483	Methyl-9-octadecanoate	$C_{19}H_{36}O_2$	37.26	WILEY229. LIB
9	37.857	Methyl octadecanoate	$C_{19}H_{38}O_2$	6.38	WILEY229. LIB
Total area (%)				99.07	

Table 6. Retention time and area of methyl ester constituent compounds low grade CPO sonotransesterification results.

in Table 6. The mass spectrum obtained at each subsequent retention time was compared to the methyl ester standard library for data similarity.

Determination of reaction rate and kinetic model

The kinetic analysis of the transesterification reaction was carried out using three different models: zero-order, pseudo-first-order, and pseudo-second-order kinetics. These models were chosen based on their relevance to heterogeneous catalytic systems with excess alcohol. The zero-order model assumes that the reaction rate is independent of reactant concentration, which is typically observed when the catalyst surface is saturated[55]. The pseudo-first-order model assumes that methanol is in large excess, making the reaction rate dependent only on triglyceride concentration[25]. The pseudo-second-order model considers the rate to be proportional to the square of the triglyceride concentration, representing more complex reaction kinetics or strong adsorption behaviour. The most suitable kinetic model was then determined by comparing the correlation coefficient (R^2) value closest to one in the kinetics model of zero order, pseudo-first-order, and pseudo-second-order kinetics.

The transesterification reactions were performed at four different temperature ranges, from 45 °C, 55 °C, 65 °C, and 75 °C, and at different times, from 15, 30, 45, and 60 min. The concentration of triglycerides over time was used to fit the three models, and the linear regression plots for each kinetic model are shown in Fig. 12. The corresponding rate constants and correlation coefficients (R^2) are summarized in Table 7.

Among the three models, the pseudo-second-order model yielded the highest R^2 values across all temperatures, ranging from 0.893 to 0.999. Although the pseudo-second-order model yielded slightly higher correlation coefficients ($R^2 = 0.999$) than the pseudo-first-order model ($R^2 = 0.998$), the latter was selected as the most appropriate model. This decision is based not only on statistical fit, but also on the reaction conditions used in this study, particularly the use of excess methanol, which favours pseudo-first-order behaviour. Moreover, the pseudo-first-order model aligns with the mechanistic understanding of base-catalysed transesterification under ultrasonic irradiation, as reported in previous studies[7,56]. Therefore, pseudo-first-order kinetics best describe the reaction mechanism in this system.

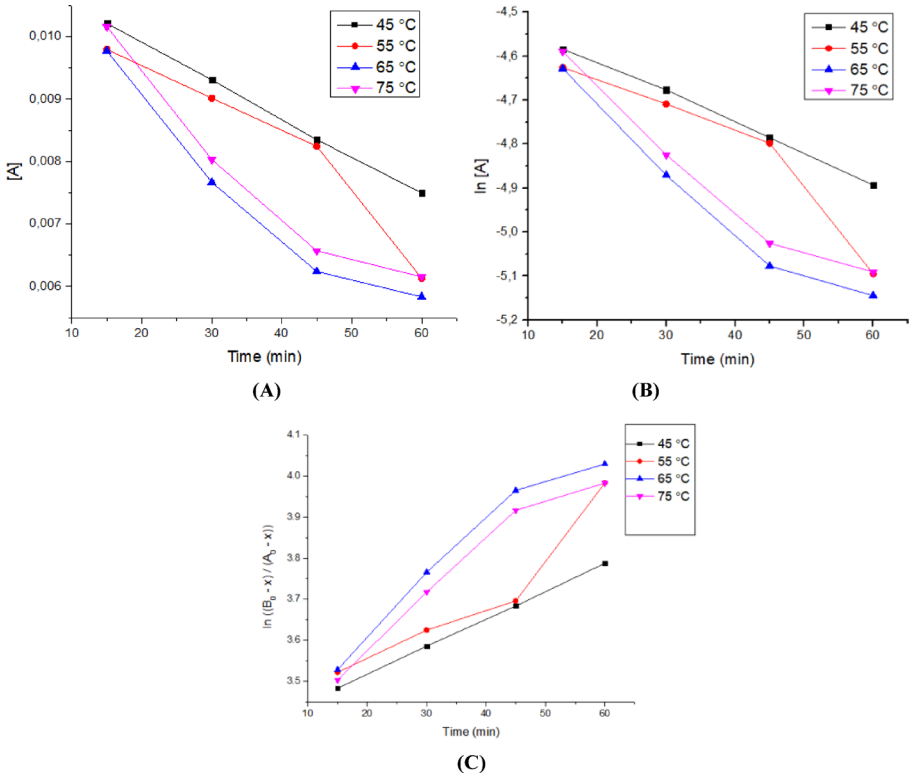

Fig. 12. Reaction curve (**A**) Order 0, (**B**) Order 1, (**C**) Order 2.

Temperature (°C)	k (L mol^{-1} min^{-1})			R^2		
	Order 0	Order 1	Order 2	Order 0	Order 1	Order 2
45	6×10^{-5}	6.9×10^{-3}	2.1×10^{-2}	0.995	0.998	0.999
55	8×10^{-1}	1.0×10^{-2}	2.9×10^{-2}	0.928	0.893	0.901
65	9×10^{-5}	1.1×10^{-2}	3.5×10^{-2}	0.924	0.949	0.948
75	9×10^{-5}	1.1×10^{-2}	3.4×10^{-2}	0.925	0.949	0.956

Table 7. The values of the reaction rate constant (k) and the correlation coefficient (R^2) based on the reaction curves of the order 0, 1, and 2.

The validity of the pseudo-first-order model was further supported by the Arrhenius plot, which showed a linear relationship between ln k vs 1/T shown in Fig. 13. The activation energy studied was limited to a temperature range of 45° to 65 °C because biodiesel yield at temperatures above 65 °C tended not to undergo significant changes. The calculated activation energy was 23.229 kJ/mol, falling within the range commonly reported for heterogeneous base catalysts (typically 20–80 kJ/mol)[23,57]. This also indicates that the reaction is chemically controlled and that the use of ultrasound enhances the rate without altering the fundamental kinetics, as previously reported[7].

Figure 13 shows a slope of −2794 and an intercept of 4.946. The activation energy value (Ea) is calculated based on the slope value of 23.229 kJ/mol. Meanwhile, the reaction's frequency factor (A) of 7×10^{-3} s^{-1} is calculated based on the intercept value. The activation energy value was much lower than that reported in the previous study, which was 57.37 kJ/mol in the Li/NaY catalyst[23] and 78.8 kJ/mol in the CaO catalyst of the reflux method[35]. Thus, the rate constants of the sonotransesterification of low grade CPO using a Na_2O/ANM catalyst (k) of $7 \times 10^{-3}.e^{(-23229/RT)}$. Based on the model fit, rate behaviour, and theoretical justification, the transesterification reaction under ultrasonic irradiation using Na_2O/ANM catalyst follows pseudo-first-order kinetics, making this model suitable for further scale-up design and optimization. These results show that using ultrasonic-assisted Na_2O/ANM catalysts in biodiesel synthesis is quite effective because it can significantly reduce the activation energy of the reaction.

Cost estimation

In this study, a low cost heterogeneous base catalyst was developed from Alpinia nigra leaves for biodiesel synthesis of low grade CPO. The calculation of the catalyst's production cost was estimated to be $ 67/kg as shown in Table 8.

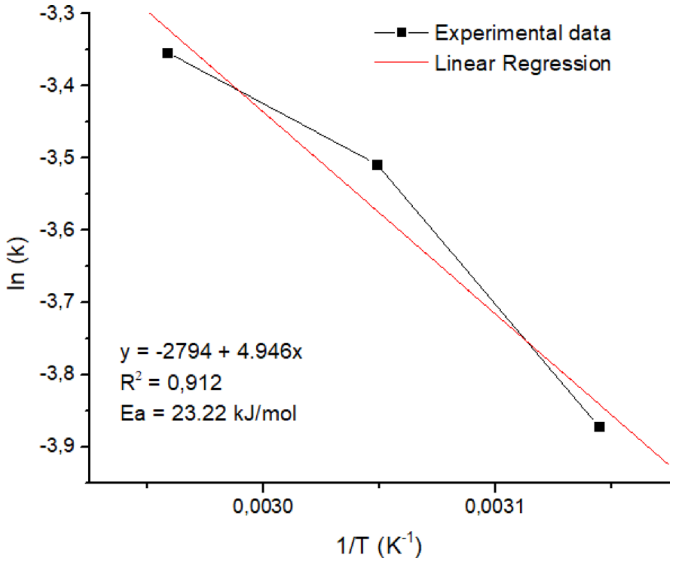

Fig. 13. Graphic 1/T versus ln k.

Step	Description	Expenses (IDR)
Low grade CPO	Waste	$0
Activation of natural mordenite		
Oven	Time (h) × units of consumed electricity × unit cost = 10 × 1 × $0.063	$0.63
Calcination	Time (h) × units of consumed electricity × unit cost = 8 × 6 × $0.063	$3.024
Reagent	1% HF + 6 M HCl + 1 M NH_4Cl = $3.09 + $2.4 + $1.06	$6.55
Impregnation		
Reagent	NaOH 30%	$2.01
Waterbath shaker	Time (h) × units of consumed electricity × unit cost = 12 × 6 × $0.063	$4.536
Oven	Time (h) × units of consumed electricity × unit cost = 4 × 6 × $0.063	$1.512
Calcination	Time (h) × units of consumed electricity × unit cost = 4 × 6 × $0.063	$1.512
Methanol		$6.2
Transesterificationn process	Cost of transesterification process = Duration of reaction (h) × units of consumed electricity × unit cost = 1 × 15 × $0.05	$0.75
	Total	$26.724

Table 8. Cost assessment of the synthesized catalyst and biodiesel synthesis.

Conclusions

The sonotransesterification of low grade Crude Palm Oil (CPO) was investigated to evaluate the effects of temperature and time on the kinetic behaviour of ultrasonic-assisted biodiesel production. The successful multi-step acid activation and impregnation of Na_2O onto activated natural mordenite (ANM) was evidenced by a reduction in the zeolite acidity from 2.605 mol/g to 0.248 mol/g, along with a uniform distribution of Na_2O on the ANM surface as observed through SEM–EDX Mapping. The catalyst demonstrated high catalytic activity in the sonotransesterification of low grade CPO, with a biodiesel yield of 80.08% at 65 °C for 65 min. Kinetic analysis indicated that the reaction followed a pseudo-first-order model, with an activation energy of 23.229 kJ/mol, a frequency factor (A) of 7×10^{-3} s^{-1}, and a reaction rate constant (k) of $7 \times 10^{-3}.e^{(-23229/RT)}$, which is lower than reported values in the previous studies. that is lower than that has been reported on the previous literature. These findings demonstrate the potential of the sonotransesterification process for efficiently converting low grade CPO into biodiesel. For further research, the challenges are improving biodiesel yield, process intensification, leaching test of the catalyst, reusability, and scale up the process.

Data availability

The datasets used and/or analysed during the current study available from the corresponding author on reasonable request.

Received: 7 February 2025; Accepted: 29 September 2025
Published online: 04 November 2025

References

1. Galvan, D., Cremasco, H., Carolina, A., Mantovani, G. & Bona, E. Kinetic study of the transesterification reaction by artificial neural networks and parametric particle swarm optimization. *Fuel* **267**, 117221 (2020).
2. Sumari, S. et al. Catalytic transesterification of kapok seed oil by dual metal oxide (Na_2O-K_2O; MgO-CaO) impregnated active-natural mordenite under ultrasonic irradiation. *Energy Sour. Part A Recover. Util Environ. Eff.* **45**, 6885–6900 (2023).
3. Pasha, M. K., Dai, L., Liu, D., Guo, M. & Du, W. Biotechnology for Biofuels An overview to process design, simulation and sustainability evaluation of biodiesel production. *Biotechnol. Biofuels* https://doi.org/10.1186/s13068-021-01977-z (2021).
4. Maheshwari, P., Belal, M., Yusuf, M. & Jaiswal, A. K. A review on latest trends in cleaner biodiesel production: Role of feedstock, production methods, and catalysts. *J. od Clean. Prod.* **355**, 131588 (2022).
5. Marina, G. et al. Science of the total environment recent advances in biodiesel production: Challenges and solutions. *Sci. Total Environ.* **794**, 148751 (2021).
6. Fattah, I. M. R., Ong, H. C., Mahlia, T. M. I., Mofijur, M. & Silitonga, A. S. State of the art of catalysts for biodiesel production. *Front. Energy Res.* **8**, 1–17 (2020).
7. Pukale, D. D., Maddikeri, G. L., Gogate, P. R., Pandit, A. B. & Pratap, A. P. Ultrasound assisted transesterification of waste cooking oil using heterogeneous solid catalyst. *Ultrason. Sonochem.* **22**, 278–286 (2015).
8. Szkudlarek, Ł, Chałupka, K., Maniukiewicz, W. & Szynkowska-j, M. I. The influence of Si / Al ratio on the physicochemical and catalytic properties of MgO / ZSM-5 catalyst in transesterification reaction of rapeseed oil. *Catalysts* **11**, 12600 (2021).
9. Sumari, S., Santoso, A. & Asrori, M. R. A review: Synthesis of biodiesel from low / off grade crude palm oil on a review: Synthesis of biodiesel from low / off grade crude palm oil on pretreatment, transesterification, and characteristics. *Orbital* https://doi.org/10.17807/orbital.v13i4.1632 (2021).
10. Sumari, S., Santoso, A. & Asrori, M. R. A review: Synthesis of biodiesel from low / off grade crude palm oil on pretreatment, transesterification, and characteristics. *Orbital* **13**, 385–391 (2021).
11. Devasan, R. et al. Microwave - assisted biodiesel production using bio - waste catalyst and process optimization using response surface methodology and kinetic study. *Sci. Rep.* https://doi.org/10.1038/s41598-023-29883-4 (2023).
12. Rattanapoltee, P., Poomprasit, D. & Kewkannetra, P. Biodiesel production via transesterification: Effect of the types of oil/alcohol and alcohol concentrations on settling behaviour of byproduct of glycerol. *Defect Diffus. Forum* **365**, 255–261 (2015).
13. Ghanbari, R., Fard, Z., Jafari, D. & Palizian, M. Biodiesel production from beef tallow using the barium oxide catalyst. *React. Kinet. Mech. Catal.* https://doi.org/10.1007/s11144-019-01672-z (2019).
14. Supamathanon, N. & Khabuanchalad, S. ScienceDirect Development of K-mordenite catalyst for biodiesel production from soybean oil. *Mater. Today Proc.* **17**, 1412–1422 (2019).
15. Patil, P., Gude, V. G., Pinappu, S. & Deng, S. Transesterification kinetics of Camelina sativa oil on metal oxide catalysts under conventional and microwave heating conditions. *Chem. Eng. J.* **168**, 1296–1300 (2011).
16. Chavez-esquivel, G. et al. State of art of alkaline earth metal oxides catalysts used in the transesterification of oils for biodiesel production. *Energies* **14**, 1–24 (2021).
17. Sumari, S. et al. Contribution of Malang quartzite-based silica in K_2O / zeolite Y catalyst for methyl ester synthesis of off grade crude palm oil. *Heliyon* **10**, e33563 (2024).
18. Busca, G. Acidity and basicity of zeolites: A fundamental approach. *Microporous Mesoporous Mater.* **254**, 3–16 (2017).
19. Busca, G. *Zeolites and Other Structurally Microporous Solids as Acid–Base Materials. Heterogeneous Catalytic Materials* Vol. 1 (2014).
20. Nurcahyani, M. U. & Sumari, S. *Alkaline Earth Metal Oxide Supported on Zeolite as a Heterogenous Basic Catalyst for Clean Fuel (Biodiesel) Production: A Mini Review* Vol. 481 01001 (2024).
21. Yang, G. & Yu, J. Advancements in basic zeolites for biodiesel production via transesterification. *Chemistry (Easton).* **5**, 438–451 (2023).
22. Martínez, S. L., Romero, R., Natividad, R. & González, J. Optimization of biodiesel production from sunflower oil by transesterification using Na_2O/NaX and methanol. *Catal. Today* **220–222**, 12–20 (2014).
23. Li, Z. et al. Recyclable Li / NaY zeolite as a heterogeneous alkaline catalyst for biodiesel production: Process optimization and kinetics study. *Energy Convers. Manag.* **192**, 335–345 (2019).
24. Lawan, I., Garba, Z. N., Zhou, W., Zhang, M. & Yuan, Z. Synergies between the microwave reactor and CaO/zeolite catalyst in waste lard biodiesel production. *Renew. Energy* **145**, 2550–2560 (2020).
25. Encinar, J. M., Pardal, A., Sánchez, N. & Nogales, S. Biodiesel by transesterification of rapeseed oil using ultrasound: A kinetic study of. *Energies* **11**, 2229 (2018).
26. Santoso, A. & ZakiyyaNur, U. U. A. T. Methyl ester synthesis of crude palm oil off grade using the K_2O/Al_2O_3 catalyst and its potential as biodiesel. *IOP Conf. Ser. Mater. Sci. Eng.* **515**, 012042 (2019).
27. Ho, W. W. S., Ng, H. K., Gan, S. & Chan, W. L. Ultrasound-assisted transesterification of refined and crude palm oils using heterogeneous palm oil mill fly ash supported calcium oxide catalyst. *Energy Sci. Eng.* **3**, 257–269 (2015).
28. Encinar, J. M., González, J. F. & Rodríguez-Reinares, A. Ethanolysis of used frying oil. Biodiesel preparation and characterization. *Fuel Process. Technol.* **88**, 513–522 (2007).
29. Ma, F. & Hanna, M. A. Biodiesel production: a review1Journal Series #12109, Agricultural Research Division, Institute of Agriculture and Natural Resources, University of Nebraska-Lincoln. 1. *Bioresour. Technol.* **70**, 1–15 (1999).
30. Qu, S. et al. Synthesis of MgO/ZSM-5 catalyst and optimization of process parameters for clean production of biodiesel from Spirulina platensis. *J. Clean. Prod.* **276**, 123382 (2020).
31. Naik, B. D. & Meivelu, U. Experimental studies on sodium methoxide supported bentonite catalyst for biodiesel preparation from waste sunflower oil. *Environ. Prog. Sustain. Energy* **39**, 13390 (2020).
32. Gharby, S. Refining vegetable oils: Chemical and physical refining. *Sci. World J.* **2022**, 6627013 (2022).
33. Angelia, D., Prestasindi, G., Permatasari, W., Redjeki, S. & Surabaya, K. Kinetics transesterification reaction of waste cooking oil into biodiesel with modified CaO. *J. Tek. Kim.* **16**, 93–100 (2022).
34. Maneerung, T., Kawi, S., Dai, Y. & Wang, C. Sustainable biodiesel production via transesterification of waste cooking oil by using CaO catalysts prepared from chicken manure. *Energy Convers. Manag.* **123**, 487–497 (2016).
35. Mierczynski, P. et al. The effect of the activation process and metal oxide addition (CaO, MgO, SrO) on the catalytic and physicochemical properties of natural zeolite in transesterification reaction. *Materials (Basel).* **14**, 2415 (2021).
36. Cadar, O. et al. Effects of thermal treatment on natural clinoptilolite-rich zeolite behavior in simulated biological fluids. *Molecules* **25**, 1–12 (2020).
37. Sumari, S., Murti, M., Santoso, A. & Asrori, M. R. SonoTransesteri fi cation of Kapok seed oil with CaO: BaO- (x : y)/ active natural zeolite catalyst. *J. Renew. Mater.* **10**, 3659 (2022).
38. Warner, T. E., Galsgaard Klokker, M. & Nielsen, U. G. Synthesis and characterization of zeolite Na-Y and its conversion to the solid acid zeolite H-Y. *J. Chem. Educ.* **94**, 781–785 (2017).
39. Side, S., Putri, S. E., Pratiwi, D. E., Rahma, A. & Rahman, A. The effect of acid treatment on the characteristics of modernite zeolite. *Sainsmat J. Ilm. Ilmu Pengetah. Alam* **12**, 114 (2023).
40. Baerlocher, C. & McCusker, L. B. *Database of Zeolite Structures*. Available on: https://www.iza-structure.org/databases Accessed: 23 October 2020 (2020).
41. Treacy, M. M. & Higgins, J. *Collection of Simulated XRD Powder Patterns for Zeolites* (Elsevier, 2007).

42. Kusuma, R. I., Hadinoto, J. P., Ayucitra, A., Soetaredjo, F. E. & Ismadji, S. Natural zeolite from Pacitan Indonesia, as catalyst support for transesterification of palm oil. *Appl. Clay Sci.* **74**, 121–126 (2013).
43. Asrori, M. R., Santoso, A. & Sumari, S. Proofing the presence of metal oxide impregnated into zeolite A without calcination: XRD and FTIR studies. *Case Stud. Chem. Environ. Eng.* **9**, 100676 (2024).
44. Wu, H., Zhang, J., Wei, Q., Zheng, J. & Zhang, J. Transesterification of soybean oil to biodiesel using zeolite supported CaO as strong base catalysts. *Fuel Process. Technol.* **109**, 13–18 (2013).
45. Shiferaw, K. A., Mathews, J. M., Yu, E., Choi, E. & Tarte, N. H. Sodium methoxide / zeolite-supported catalyst for transesterification of soybean waste cooking oil for biodiesel production. *Inorganics* **11**, 163 (2023).
46. Yan, L., Fu, T., Wang, J. & Narkhede, N. Evolution of the pore and framework structure of NaY zeolite during alkali treatment and its effect on methanol oxidative carbonylation over a CuY catalyst. *J. Chem. Res.* https://doi.org/10.1177/1747519820915418 (2020).
47. Intarapong, P., Iangthanarat, S. & Phanthong, P. Activity and basic properties of KOH / mordenite for transesterification of palm oil. *J. Energy Chem.* **22**, 690–700 (2013).
48. Irawan, W. & Amri, A. Penentuan Kadar bleaching earth dan Phosporic acid pada Proses Degumming dan bleaching crude palm oil. *J. Bioprocess Chem. Environ. Eng. Sci.* **2**, 1–14 (2021).
49. Kulkarni, V., Jain, S., Khatri, F. & Thulasi, V. Degumming of Pongamia Pinnata by acid and water degumming methods Degumming of Pongamia Pinnata by Acid and Water Degumming Methods. (2016).
50. Deffense, E. From organic chemistry to fat and oil chemistry. *OCL - Ol. Corps Gras. Lipides* **16**, 14–24 (2009).
51. Pandiangan, K. D. et al. Study on the reaction parameters on transesterification of rubber seed oil using MgO / zeolite-a catalyst. *Trends Sci.* **20**, 6480 (2023).
52. Cheng, S. F., Chuah, C. H., Ngan, M. A. & Hock, C. C. Kinetics study on transesterification of palm oil. *J. Oil Palm Res.* **16**, 91–100 (2015).
53. Farouk, S. M., Tayeb, A. M., Osman, R. M. & Hamid, S. M. S. A. Sustainable production of biodiesel from waste cooking oil using magnesium oxide nano catalyst: An optimization study. *Sci. Rep.* https://doi.org/10.1038/s41598-024-71930-1 (2024).
54. Meher, L. C., Vidya Sagar, D. & Naik, S. N. Technical aspects of biodiesel production by transesterification - a review. *Renew. Sustain. Energy Rev.* **10**, 248–268 (2006).
55. Liu, X., He, H., Wang, Y., Zhu, S. & Piao, X. Transesterification of soybean oil to biodiesel using CaO as a solid base catalyst. *Fuel* **87**, 216–221 (2008).
56. Kojima, Y. & Takai, S. Transesterification of vegetable oil with methanol using solid base catalyst of calcium oxide under ultrasonication. *Chem. Eng. Process. - Process Intensif.* **136**, 101–106 (2019).
57. Pavlović, S. M., Marinković, D. M., Kostić, M. D. & Janković-častvan, I. M. A CaO / zeolite-based catalyst obtained from waste chicken eggshell and coal fly ash for biodiesel production. *Fuel* **267**, 117171 (2020).

Acknowledgements

The author would like to thank the Ministry of Education, Culture, Research, and Technology (KEMDIK-BUDRISTEK) and the Institute for Research and Community Service (LPPM) UM, for the opportunity and support for the implementation of DRTPM research with contract number: 11.6.138/UN32.14.1/LT/2024.

Author contributions

Maria Ulfa Nurcahyani: Writing an original draft, Visualization, Methodology, Investigation, Sumari Sumari: Writing an original draft, Project administration, Methodology, Investigation, Funding acquisition, Conceptualization, Aman Santoso: Validating, Supervision Project Administration, Conceptualization, Galih Satrio Putra: Writing – review & editing, Visualization, Validation, Evilia Wahyuning Nur A'issyah: Methodology and Investigation, Visualization, Validation, Ahmat Fanani Hidayatulloh: Methodology and Investigation.

Funding

Ministry of Education, Culture, Research, and Technology (KEMDIKBUDRISTEK) and the Institute for Research and Community Service (LPPM), 11.6.138/UN32.14.1/LT/2024,11.6.138/UN32.14.1/LT/2024

Declarations

Competing interests

The authors declare that they have no known competing financial interests or personal relationships that could have appeared to influence the work reported in this paper.

Additional information

Correspondence and requests for materials should be addressed to S.S.

Reprints and permissions information is available at www.nature.com/reprints.

Publisher's note Springer Nature remains neutral with regard to jurisdictional claims in published maps and institutional affiliations.